Structural Engineering and Mechanics, Vol. 6, No. 6 (1998) 693-710
DOI: http://dx.doi.org/10.12989/sem.1998.6.6.693

Studies on post-tensioned and shaped space-truss domes

Lewis C. Schmidt† and Hewen Li‡

Department of Civil and Mining Engineering, University of Wollongong, NSW 2500, Australia

Abstract. This paper concerns studies on the shape formation of post-tensioned and shaped steel domes. The post-tensioned and shaped steel domes, assembled initially at ground level in an essentially flat condition, are shaped to a curved space form and erected into the final position by means of a post-tensioning technique. Based on previous studies on this shape formation principle, three post-tensioned and shaped steel domes have been constructed. The results of the shape formation tests and finite element analyses are reported in this paper. It is found that the first two test domes did not furnish a part-spherical shape as predicted by finite element analyses, because the movements of some mechanisms were not controlled sufficiently. With a revised post-tensioning method, the third dome obtained the theoretical prediction. The test results of the three post-tensioned and shaped domes have shown that a necessary condition to form a desired space shape from a planar layout with low joint stiffnesses is that the movements of all the existing mechanisms must be effectively controlled as indicated by the finite element analysis. The extent of the maximum elastic deformation of a post-tensioned and shaped steel structure is determined by the strength of the top chords and their joints. However, due to the semi-rigid characteristic of the top chord joints, the finite element analyses cannot give a close prediction for the maximum elastic deformations of the post-tensioned and shaped steel domes. The results of the current studies can be helpful for the design and construction of this type of structure.

Key words: space structure; finite element; post-tensioning; construction.

1. Introduction

Post-tensioned and shaped space trusses are a type of recently developed steel structure which is capable of being shaped to a curved space shape and erected into the final position from a planar layout by means of post-tensioning. The basic structural module of the post-tensioned and shaped space truss is the so-called Single-Chorded Space Truss (SCST), a truss with a single-layer of chords, together with out-of-plane web members. In the initial planar configuration, the SCST provides near mechanisms that can be readily shaped with relatively small post-tensioning forces, as flexure occurs only in the top chords. By means of post-tensioning, the SCST can be deformed to the desired space shape. After a self-locking process for certain members that are inserted too short initially, the SCST becomes a stable structure and can carry significant loads (Schmidt 1989).

The post-tensioned and shaped steel domes studied in this paper belong to the Space-Shape-

† Professor
‡ Research Student

Based type (Li and Schmidt 1997), i.e., the planar layout of the dome is determined by its desired space shape. Previous studies have verified the possibility of shaping a Space-Shape-Based dome from a planar layout by post-tensioning (Schmidt and Li 1995a, b). In this paper attention is paid to the construction of the test domes. The studies in this paper include three Space-Shape-Based post-tensioned and shaped domes. In the following sections, they are referred to as SSBD 1 (Space-Shape-Based Dome 1), SSBD 2 and SSBD 3, respectively.

The principal objective of the studies on SSBD 1 is to form a true part-spherical dome from a flat condition. The shape formation studies of SSBD 1 can be divided into the following three parts: (1) establishing the space geometric model and the planar geometric model by means of an optimization method; (2) shape formation analysis by means of the finite element method; and (3) shape formation test based on the theoretical work.

The principal objective of the studies on SSBD 2 is to investigate its maximum elastic deformation extent. The studies on SSBD 2 include shape formation analysis by means of the finite element method, and the shape formation test based on the results of the analyses.

The principal objective of the studies on SSBD 3 is to form a uniform-gap dome to its maximum elastic deformation extent. The shape formation studies of SSBD 3 include the following three parts: (1) development of a post-tensioning method that can effectively control all the existing mechanisms in the planar layout; (2) shape formation analysis by means of the finite element method; and (3) shape formation test.

2. Theoretical analyses of SSBD 1

2.1. Space geometric model and planar geometric model of SSBD 1

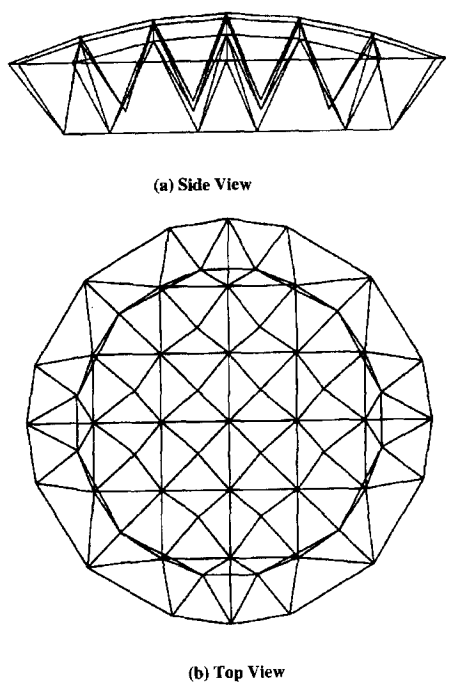

Fig. 1 Space geometric model of SSBD 1

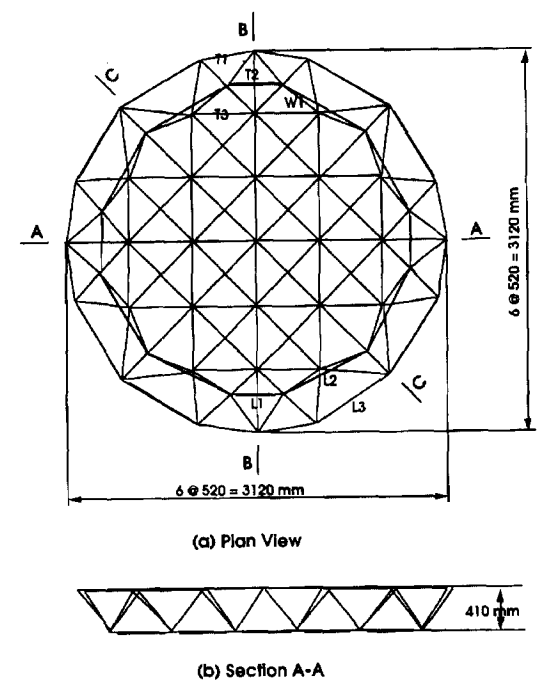

Fig. 2 Planar layout (planar geometrical model) of SSBD 1

Table 1 Coordinates of joints for SSBD 1 (mm)

Joint	*X*	*Y*	*Z*	Joint	*X*	*Y*	*Z*
1	0.0	1560.0	0.0	11	520.0	0.0	0.0
2	447.4	1448.0	0.0	12	1040.0	0.0	0.0
3	0.0	1040.0	0.0	13	1560.0	0.0	0.0
4	520.0	1040.0	0.0	14	230.2	1266.9	−410.0
5	1096.4	1096.4	0.0	15	260.0	780.0	−375.0
6	0.0	520.0	0.0	16	901.0	901.0	−410.0
7	520.0	520.0	0.0	17	260.0	260.0	−375.0
8	1040.0	520.0	0.0	18	780.0	260.0	−375.0
9	1448.0	447.4	0.0	19	1266.9	230.2	−410.0
10	0.0	0.0	0.0				

Note: The positions of the joints are shown in Fig. 3.

The proposed span of SSBD 1 is 3080 mm; the height is 550 mm; the rise is 220 mm; and the radius of the dome surface is 5390 mm. According to the above parameters, the dome is meshed with 60 top chords and 96 web members by means of an optimization method (Schmidt and Li 1995a). The length of a regular top chord is 520 mm and the length of a regular web member is 525 mm. The proposed space shape (space geometric model) of SSBD 1 is shown in Fig. 1.

The planar geometric model (planar layout) of SSBD 1, as shown in Fig. 2, is derived from the space geometric model. The joint coordinates in a quarter planar layout are given in Table 1 with the joint positions shown in Fig. 3. It can be seen that the layout of the members in SSBD 1 is highly regular: 36 among 60 top chords (60%), and 80 among 96 web members (84%) have a regular length (the greater the number of chords and members involved in such a structure, the higher the degree in regularity), and there are only 4 types of top chords and 6 types of web members. The high degree in regularity can provide economical advantages in simplifying the fabrication.

In the initial planar layout, the total number of top chords and web members b is 156; the total number of joints j is 61 (37 surface joints and 24 web joints). Assuming a pin-jointed truss and that the number of overall restraints r is 7 (the minimum number to prevent a

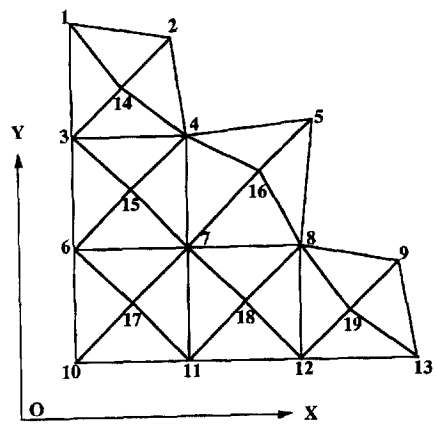

Fig. 3 Joint positions of a quarter planar layout of SSBD 1

structure from rigid body movement is 6), and substituting them into the Maxwell criterion $R=b-(3j-r)$, and $R-S+M=0$ (Calladine 1978), it is found that the structure includes 20 independent mechanisms ($M=20$, $R=-20$) before the post-tensioning operation (as the number prestress states $S=0$). This means that 20 members need to be added to the planar layout in order to form a stable structure ($M=0$) that is just statically determinate.

2.2. Post-tensioning method of SSBD 1

The post-tensioning method employed in this paper is to tension strands along the gap members in a planar layout (SCST). The planar layout (Fig. 2) is assembled with gap members, which comprise shorter tubes and strands that pass through the tubes and relevent joints. As the strands are tensioned by hydraulic jacks or other equipment, the gap members will shorten at the gap locations. As a result, the planar layout is shaped into a curved space shape and erected into its final position. The principal factors of a post-tensioning method are to select the positions of the gap members and to determine the values of the gaps, because they will determine the final shape of the structure.

Comparing the space geometric model with the planar geometric model, it can be found that the distance changes between the joints, to which there is no direct member to connect, are significant, if the planar layout is deformed to a curved space shape. However, only a few are necessary to suppress mechanisms for the required shape formation of the post-tensioned and shaped space dome among the possible distance changes, according to the Maxwell criterion (Calladine 1978). The principal objective of the post-tensioning method is to select the M independent mechanisms from the many possible distance changes. Obviously, several potential post-tensioning layouts exist in the given planar arrangement of members.

The selection of the most convenient post-tensioning method, both from a practical and from a structural point of view, is still an open question. However, the basic criterion for selecting a post-tensioning method should be whether a structure can obtain its desired space shape by inserting members too short and then closing the gaps, and whether large stresses are induced during the post-tensioning process. To investigate the feasibility of a proposed post-tensioning method, a finite element analysis is helpful. The results of a finite element analysis will indicate whether the planar layout can be deformed to the desired space shape by the proposed post-tensioning method, whether large stresses are induced during the post-tensioning process, and give the values of the post-tensioning forces.

Based on the number of mechanisms ($M=20$), a post-tensioning method, as shown in Fig. 2, is proposed for SSBD 1. Eight peripheral gap top chords and twelve short bottom chords are added to the planar layout as indicated with thick lines in Fig. 2. The gap members comprise shorter tubes and strands that pass through the tubes and through the connecting joints. The initially too-short tubes are used to create pre-defined gaps, while the strands are used to close the gaps. If all the gaps close after the post-tensioning operation, the total number of members b will become 176, while the total number of joints j remains 61. In this case, $M=0$ and $R=0$, i.e., the dome has no mechanism left after post-tensioning. If additional restraints are added, the dome will become statically indeterminate ($R>0$). The above results show that the proposed post-tensioning method satisfies the mechanism condition (Schmidt and Li 1995b).

2.3. Finite element analyses of SSBD 1

A finite element analysis is used to investigate the feasibility of the proposed post-

tensioning method. Because the deformed shape of the post-tensioned and shaped dome is different from its original flat geometry, the shape formation process induces large deformations, and the analysis is highly nonlinear geometrically and may also be materially nonlinear. To consider the nonlinearity of the structural behaviour during shape formation, the program MSC/NASTRAN (1995) is employed. The analysis commences with the initial configuration of the planar layout in which all the top chords are horizontal.

The first step in the finite element analysis is to establish an accurate finite element model. However, it is difficult to achieve such an objective because SSBD 1 involves near-mechanisms. During the shape formation stage, SSBD 1 involves genuine mechanisms according to the Maxwell criterion (Calladine 1978), but it also involves the non-stress-free distortion of what are essentially rigid frames because of the moment resisting nature of the top chord joints. Because the structural behaviour of SSBD 1 is between those of a truss and a frame, it is analyzed with two finite element models. In model 1, all members, including top chords, web members and bottom chords, are modelled as pin-connected rod elements. There are a total of 61 joints and 176 rod elements in model 1. In model 2, the non-gap top chords are modelled as a series of straight and uniform beam elements. The short members and web members are modelled as pin-connected rod elements. There are a total of 61 joints, 60 beam elements and 116 rod elements in model 2. Because SSBD 1 involves near-mechanisms, the joint eccentricitices are omitted in the above numerical analyses. This is because the increase of additional joints and members, which are necessary to consider the joint eccentricities in a finite element analysis, will result in a difference between the number of theoretical and practical mechanisms, according to the Maxwell criterion (Calladine 1978).

In the finite element analyses, the geometry and material properties of elements are the same as in the test dome. The top chords in SSBD 1 are made of $13\times13\times1.8$ mm square hollow steel (SHS) tubes, while the web members are made of 13.5×2.3 mm circular hollow steel (CHS) tubes. The properties of the steel are as follows: Young's modulus E=200 GPa, Poisson's ratio ν=0.3; the yield stress is 450 MPa for the top chords, and 440 MPa for the web members, determined according to the experimental results.

One problem in the shape formation analysis is how to simulate the closing of the gaps caused by inserting members too short. Here, the closing of the gaps in the bottom chords and some top chords is simulated with a thermal load. The too-short members, as shown in Fig. 2, are given fictitious different thermal coefficients in proportion to the values of gaps, as listed in Table 2. The top and bottom joints that connect the short members are given a uniform thermal load of -10°C. The thermal load is divided into 20 load steps in the finite element analyses.

The results of finite element analyses show that both models achieve the space shape obtained by an optimization method (Schmidt and Li 1995a), with tolerances within 1%. At the last load step (step 20), the overall height of SSBD 1 is 548 mm and the surface rise is 218 mm. The surface span is 3080 mm, and all surface joints are within the space formed by the two spheres with the radii of 5382 mm and 5396 mm, respectively.

Table 2 Gaps and thermal coefficients of gap-members in SSBD 1

	L1	L2	L3
Original length (mm)	460.4	764.1	738.1
Value of gap (mm)	36.4	64.6	12.3
Thermal coefficient	0.00790	0.00846	0.00167

Note: The positions of the members are shown in Fig. 2.

At the last load step (step 20), the maximum theoretical post-tensioning force for closing a gap is 0.065 N in model 1, and is 4.4 kN in model 2. With model 1, the maximum axial force is 0.054 kN and occurs in member T1 in Fig. 2. With model 2, the maximum axial force is 2.2 kN and occurs in member T2 in Fig. 2. The flexural stresses are almost zero in model 1 and are greater than the yield stress in model 2.

3. Shape formation test of SSBD 1

The experimental planar layout of SSBD 1, as shown in Fig. 4, is a modified Single Chorded Space Truss (SCST), a space truss with a single layer of chords, together with out-of-plane web members. As shown in Fig. 3, the two top chords and four web members in the non-regular pyramidal units are adjusted to suit the circular boundary of SSBD 1. The planar layout was assembled on the floor from a single-layer mesh grid of top chords and pyramidal units of web members. All of the non-gap top chords of the dome were continuous. One series of continuous chords was placed over the other continuous series, and bolted together with 6 mm high tensile cap screws. The ends of the continuous top chords were bent in the horizontal plane in order to form the quadrilateral meshes shown in Fig. 3. Four web members were welded to a bottom joint to form a pyramidal unit. The pyramidal unit was also bolted to the top chords with 6 mm high tensile cap screws.

The tubular bottom chords were also made of $13\times13\times1.8$ SHS steel tube and were assembled to the planar layout by high tensile strands. For simplicity, only four high tensile strands were used to assemble the 12 shorter tubular bottom chords to the planar layout. As shown in Fig. 5, each tensile strand passed through four edge bottom joints and through three shorter tubes.

Fig. 4 Planar Layout of Test SSBD 1

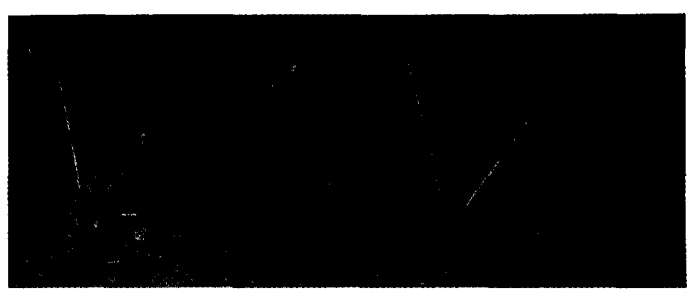

Fig. 5 Gaps Created by Shorter Bottom Chords and a Sliding Gap Top Chord in Planar Layout of SSBD 1

To reduce arching of the bottom chords during post-tensioning, each end of a bottom chord had a chamfer. The angles of the chamfers were calculated according to the results of the finite element analysis, with the assumption that the faces of the bottom joints would "just touch" with the ends of the bottom chords at the end of the post-tensioning operation. The angles of the chamfers for L1 and L2 in Fig. 2 were 72.7° and 79.7°, respectively.

The gap top chords were made of two different size SHS steel tubes as shown in Fig. 5. The smaller rigid tube could slide freely in the larger one. During the shape formation test, the gap top chords were not tensioned. It was expected that the overall length of such combined gap top chords could change to the desired value as the gaps in the bottom chords were closed.

The post-tensioning procedure began with the planar layout in its initial position, i.e., all the top chords were flat. A hydraulic jack was used to apply an axial force to the individual strands that each passed through three tubular bottom chords. During the post-tensioning procedure, the supports of the dome were the peripheral bottom joints, which were free to slide horizontally and to rotate. The average of the four post-tensioning forces that each closed three gaps in the bottom chords was 2.1 kN. Therefore, the average post-tensioning force for closing a gap was 0.7 kN.

It has been shown that the theoretical post-tensioning force for closing a gap was 0.065 kN with model 1 and 2.2 kN with model 2. Compared with the theoretical post-tensioning force, the practical post-tensioning force was between the predictions given by model 1 (rod top chords and rod web members) and model 2 (beam top chords and rod web members). This indicates that the practical joints in the test dome were semi-rigid.

The test SSBD 1 is shown in Fig. 6. Its theoretical and experimental surface shapes and positions are shown in Fig. 7. The principal dimensions of SSBD 1 are listed in Table 3. It was found that the test dome did not have a true part-spherical surface. In plan, it was more like an oval due to the curvatures along the two directions A and B in Fig. 2 not being the same. Both the periphery of the top surface and the periphery formed by the bottom chords was not a circle but an ellipse. The overall height of the experimental dome was 568 mm, and compared with the theoretical overall height of 548 mm, the difference was 3.6%.

The difference between theoretical and experimental space shapes of SSBD 1 can be attributed to the existence of more mechanisms in SSBD 1 than the mechanisms practically controlled by the post-tensioning operation, and the slight position difference in the levels of the top chords in the two directions. The gap top chords, which were expected to slide to the desired length when the gaps in the bottom chords closed, actually had different lengths at the

Fig. 6 Space Shape of Test SSBD 1

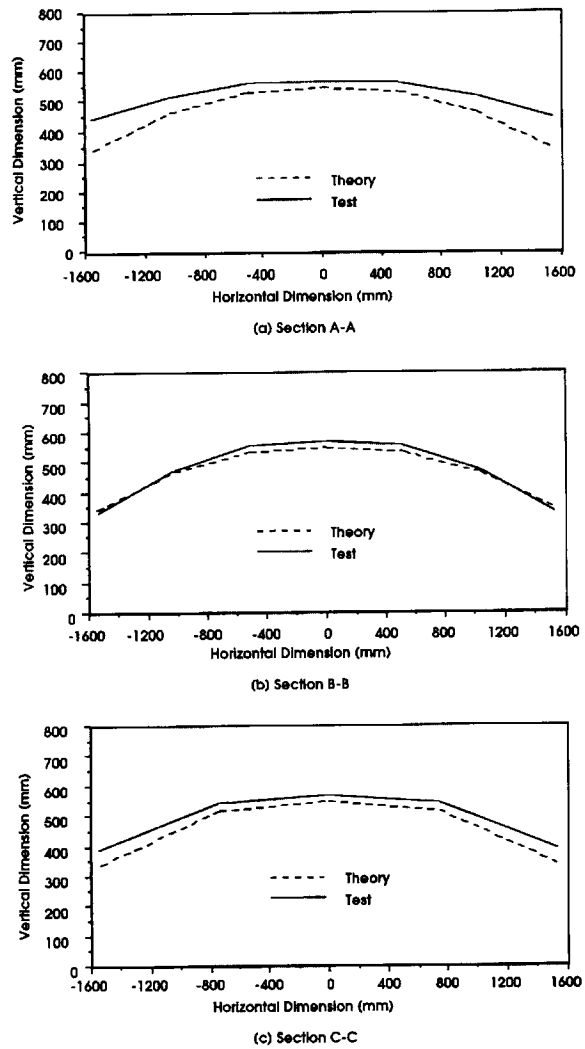

Fig. 7 Surface shapes and positions of SSBD 1 along different directions (Section A-A, B-B and C-C are defined in Fig. 2)

Table 3 Span dimensions of SSBD 1 (mm)

	Thory		Test	
Span	Surface Periphery	Bottom Periphery	Surface Periphery	Bottom Periphery
Span A	3080	2352	3110	2390
Span B	3080	2352	3063	2335
Span C	3078	2350	3080	2365

Note: The directions of the spans are shown in Fig. 2.

end of the post-tensioning operation. This meant that the movements of the eight mechanisms in the gap top chords had not been efficiently controlled. Because the top chords had bolt holes at joint positions, the top joints were weaker than the members, and the structural behavior of SSBD 1 was more like that of a pin-jointed structure. When the mechanisms

were not sufficiently controlled, such a planar layout could not be deformed to the space shape predicted with the beam top chord finite element model. Because the top chords were continuous and one series of continuous chords was placed over the other continuous series, the bending moments in the upper layer of top chords were larger than those in the lower one. In a structure in which independent mechanisms exist, such a structural difference is enough to induce a significant difference in deformations. As a result, the curvatures along the two directions A and B were not the same. The planar layout could not be deformed to a true part-spherical surface as predicted by theoretical analyses in which all mechanisms were effectively controlled.

It was found that the space shape of SSBD 1 was achieved principally by the in-plane rotation and the out-of-plane flexural deformation of top chords at the joints. The segments of the top chords between panels remained straight axially, although square meshes of top chords deformed to rhombic forms as can be seen in Fig. 6. All the deformations in test SSBD 1 were within the yield limit of materials, because the release of the post-tensioning force caused the dome to flatten to a planar layout again. Although the experimental flexural stresses were unknown, the stresses were different from the theoretical predictions. While the finite element analysis using beam top chord elements overestimated the flexural stresses (the theoretical flexural stresses in most of the top chords are greater than the yield stress of the material), the finite element analysis using rod top chord elements underestimated them (the theoretical flexural stresses in all the members are zero). To obtain a better description for the post-tensioned and shaped steel structures, a finite element program that considers the semi-rigid characteristic of the top joints is desirable.

4. Shape formation analysis and test of SSBD 2

The planar layout of SSBD 2 is the same as that of SSBD 1, except the eight gap top chords are removed. The principal objective of the studies on SSBD 2 is to investigate its maximum elastic deformation extent.

4.1. Finite element analysis of SSBD 2

Like SSBD 1, the shape formation analysis of SSBD 2 is also carried out using the program MSC/NASTRAN (1995). The geometry and material properties of elements are the same as that in SSBD 1. Because there are eight mechanisms existing in SSBD 2, the all-rod element model cannot furnish a unique deformed shape. Therefore, all top chords are modelled as a series of straight and uniform beam elements. All the web members and bottom chords are modelled as pin-connected rod elements. There are a total of 61 joints, 60 beam elements, and 108 rod elements in the finite element model. The analysis commences with the initial configuration of the planar layout in which all the top chords are horizontal.

The thermal coefficients for the bottom chords are the same as listed in Table 2. Also, the bottom joints that connect the bottom chords are given a uniform negative thermal load. Because the objective of the shape formation analysis of SSBD 2 is to investigate its maximum elastic deformation extent, the values of the gaps are unknown. In the finite element analysis, a large uniform negative thermal load is given. The thermal load of $-18^{\circ}C$ is divided into 50 load steps in the finite element analysis. At the last load step (step 50), the maximum axial force in the top chords is -23.4 kN and occurs in member T3 in Fig. 2. The

maximum axial force in the web members is −22.9 kN and occurs in member W1 in Fig. 2. Again, most of the flexural stresses are beyond the yield strength.

At the last load step (step 50), the lengths of the gap members in L1 and L2 in Fig. 2 are 381.7 mm and 540.3 mm, respectively. The overall height of SSBD 2 is 610 mm and the surface rise is 350 mm. The surface spans along directions A and B are 2998 mm, and the surface span along direction C is 3035 mm (because the planar layout is designed for SSBD 1, the change in gap values in SSBD 2 cannot result in a part-spherical surface). The maximum post-tensioning force for closing a gap is 12 kN.

4.2. Shape formation test of SSBD 2

Because it is unknown if the finite element analysis can give a reliable prediction for the extent of the maximum elastic deformation, the values of the gaps in SSBD 2 were increased step by step (i.e., the lengths of the gap members were reduced step by step). The lengths of the gap members at different steps are listed in Table 4. The lengths of gaps members at step 4 were equal to those obtained in the last load step (step 50) in the above finite element analysis. In the first three steps, the space shape of SSBD 2 in plan was still an oval, and the member

Table 4 Gap member lengths of SSBD 2 at different steps (mm)

	Original	Step 1	Step 2	Step 3	Step 4
L1	460.5	418.0	415.5	403.0	381.8
L2	764.1	699.0	679.0	613.5	540.3

Note: The positions of the members are shown in Fig. 2.

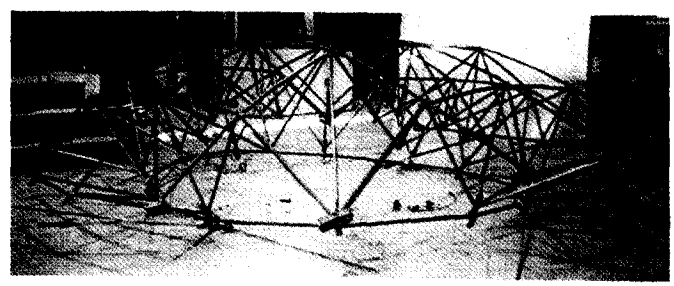

Fig. 8 Space shape of test SSBD 2

Fig. 9 Fractured top chord at a joint of test SSBD 2

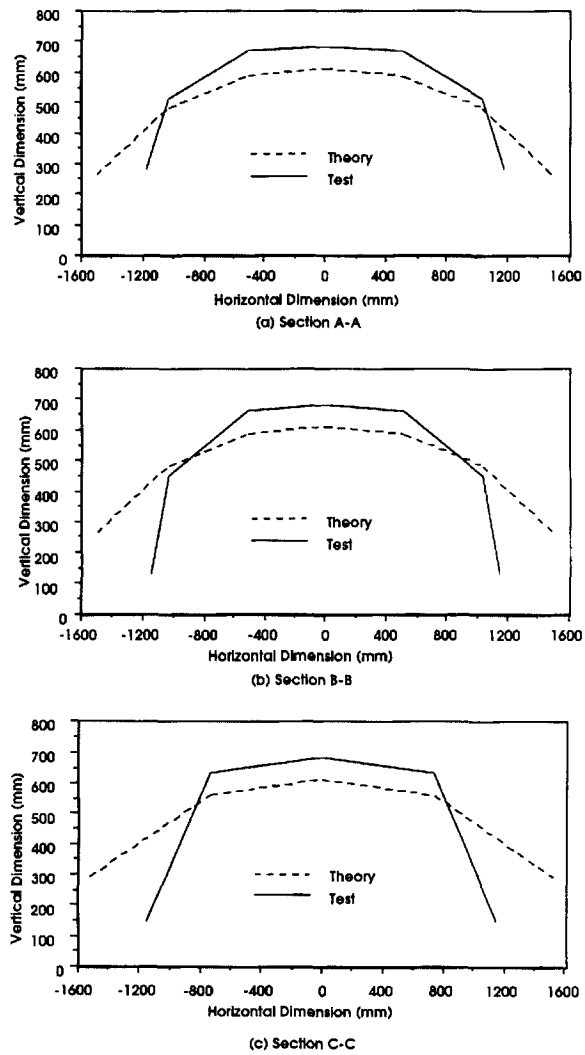

Fig. 10 Surface shapes and positions of SSBD 2 along different directions (Section A-A, B-B and C-C are defined in Fig. 2)

deformations were within the elastic range. However, at the end of step 4, two continuous upper top chords yielded at four joints. This meant that SSBD 2 reached its maximum elastic deformation due to yielding and subsequent fracture of the top chords at the joints.

The space shape of SSBD 2 at the end of the step 4 is shown in Fig. 8. The detail of a failed top chord at top joint is shown in Fig. 9. One of the yielded top joints is shown as joint 4 in Fig. 3 and the other three joints had the same or symmetrical position as joint 4 in Fig. 3. The average of the four post-tensioning forces that each closed three gaps in the bottom chords was 4.6 kN. Again, the practical post-tensioning force was different from the post-tensioning force given by the finite element analysis (beam top chords and rod web members).

The theoretical and experimental surface shapes and positions of SSBD 2 are shown in Fig. 10. The principal dimensions of SSBD 2 are listed in Table 5. It was found that the test dome

Table 5 Span dimensions of SSBD 2 (mm)

	Theory		Test	
Span	Surface Periphery	Bottom Periphery	Surface Periphery	Bottom Periphery
Span A	2998	2140	2360	2005
Span B	2998	2140	2285	1730
Span C	3035	2233	2310	1963

Note: The directions of the spans are shown in Fig. 2.

did not have a true part-spherical surface. The central part of SSBD 2 was almost flat, and the curvatures along the two directions A and B in Fig. 2 were not the same and were not smooth. In plan, the periphery of the top surface and the periphery formed by the bottom chords were ellipses. The overall height of the experimental dome was 682 mm, and its difference with the theoretical overall height was 12%.

As explained previously, the difference between the theoretical and experimental space shapes can be attributed to the existence of the additional mechanisms, and the slight position difference in the top chords along the two directions. The large difference in overall height can be attributed to the top chords yielding at four joints. Because two top chords yielded at the four joints near to the edge, the post-tensioned forces applied to the bottom chords cannot be efficiently transferred to the central part, and the deformations of the edge pyramids were large. As a result, the central area was relatively flat and the edge part was almost vertical in SSBD 2.

The test SSBD 2 reached its maximum elastic deformation extent due to two top chords yielding and fracturing at four joints. This failure demonstrated that the maximum elastic deformation extent of such a post-tensioned and shaped dome depended on the strength of the top chords. Because the top chords were weakened by the bolt holes at the joints, they failed at joint positions.

5. Shape formation analyses and test of SSBD 3

5.1. Post-tensioning method of SSBD 3

The planar layout of SSBD 3 is the same as that of SSBD 1. Because the post-tensioning method used in SSBDs 1 and 2 cannot effectively control the movements of the existing mechanisms, a revised post-tensioning method is proposed for SSBD 3.

As indicated previously, the number of independent mechanisms is 20 in the initial planar layout. In the new post-tensioning method, all the twenty independent mechanisms are controlled with short bottom chords and cables. The twenty short chords are connected to the bottom joints by four cables as indicated with thick lines in Fig. 11. SSBD 3 is post-tensioned with the four cables along the two directions A and B in Fig. 11. If all the 20 gaps close, then no mechanism is left after the post-tensioning operation. Because all the 20 short bottom chords are post-tensioned, the new post-tensioning method effectively controlled all of the existing mechanisms in the planar layout.

5.2. Finite element analyses of SSBD 3

SSBD 3 is analyzed with two finite element models in which all the top chords are

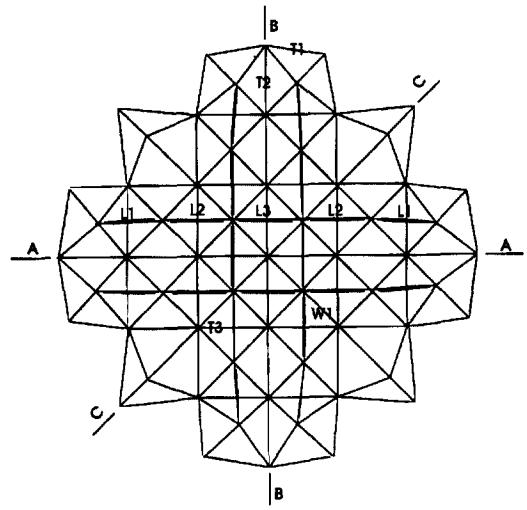

Fig. 11 Post-tensioning method for SSBD 3

horizontal initially. In model 1, all members, including top chords, web members and bottom chords, are modelled as pin-connected rod elements. There are a total of 61 joints and 176 rod elements in model 1. In model 2, the top chords are modelled as a series of straight and uniform beam elements. The bottom chords and web members are modelled as pin-connected rod elements. There are a total of 61 joints, 60 beam elements and 116 rod elements in model 2.

In the finite element analyses, the closing of the gaps in the bottom chords is simulated with a thermal load. Because the objective of the shape formation analysis of SSBD 3 is to investigate its maximum elastic deformation extent, all the gaps in SSBD 3 are given the same value of 150 mm (about 30% of their original lengths). The bottom joints that connect the bottom chords are given a uniform negative thermal load of $-40^{\circ}C$. The too-short members are given different artificial thermal coefficients in proportion to their original lengths, as listed in Table 6.

The thermal load of $-40^{\circ}C$ is divided into 80 load steps in the finite element analysis. At the last load step (step 80), the theoretical post-tensioning force for closing the five gaps on a cable is 1.2 kN in model 1, and is 46 kN in model 2. With model 1, the maximum axial force in the top chords is -0.281 kN, and occurs in top chord T3 in Fig. 11. The maximum axial force in the web members is 0.344 kN, and occurs in member W1 in Fig. 11. With model 2, the maximum axial force in the top chords is -16.9 kN and occurs in member T3 in Fig. 11. The maximum axial force in the web members is 22 kN, and occurs in member W 1 in Fig. 11. Again, the flexural stresses are almost zero in model 1, and beyond the yield stress in model 2.

Table 6 Gaps and thermal coefficients of gap-members in SSBD 3

	L1	L2	L3
Original length (mm)	520.0	520.0	489.0
Value of gap (mm)	150.0	150.0	150.0
Thermal coefficient	0.00722	0.00722	0.00768

Note: The positions of the members are shown in Fig. 11.

At the last load step (step 80), the overall height of SSBD 3 is 972 mm, and the surface spans along the two directions A and B in Fig. 11 are the same with a value of 2609 mm. The surface span along direction C in Fig. 11 is 2310 mm (with such a planar layout, uniform gaps cannot result in a part-spherical surface). Due to the large deformations, all the bottom joints are raised in space, and the edge top joints become the lowest points. The surface rise is equal to the overall height in SSBD 3.

5.3. Shape formation test of SSBD 3

SSBD 3 had the same planar layout as SSBD 1, but a different post-tensioning method. The 20 shorter tubular bottom chords were assembled to the planar layout by four high tensile strands. As shown in Fig. 11, each tensile strand passed through six bottom joints and through five shorter tubes. The tubular bottom chords were made of $13\times13\times1.8$ SHS steel tube. To reduce arching of each of the bottom chords during post-tensioning, each end of a

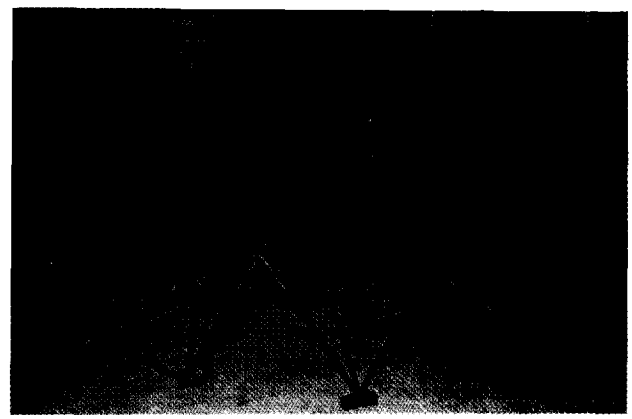

Fig. 12 Space shape of test SSBD 3

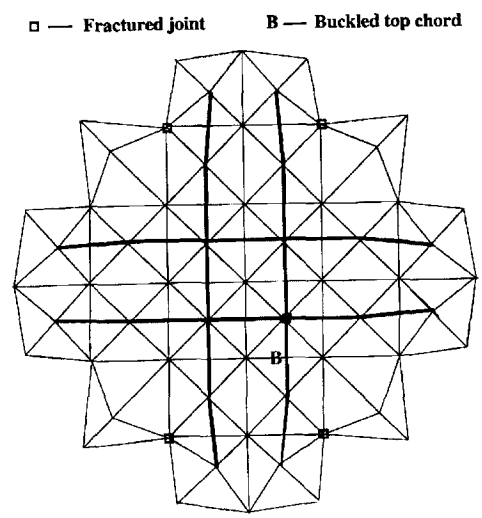

Fig. 13 Positions of fractured joints and the buckled top chord

bottom chord had a chamfer. All the bottom chords in SSBD 3 were cut 150 mm shorter than the planar distance between the bottom joints to which they were connected. The lengths of the bottom chords were equal to those obtained in the last load step (step 80) in the previous finite element analyses.

The post-tensioning procedure began with the planar layout in its initial position, i.e., all the top chords were flat. A hydraulic jack was used to apply an axial force to the individual strand that passed through the five tubular bottom chords. At the initial stage of the post-tensioning procedure, the supports of the dome were the peripheral bottom joints which were

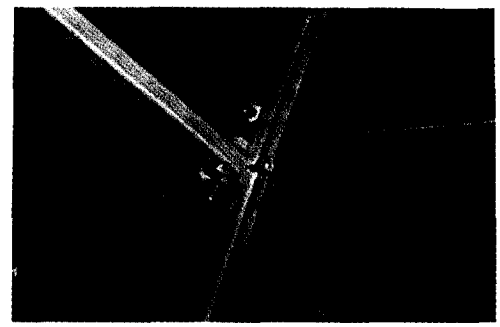

Fig. 14 A fractured top joint in test SSBD 3

Fig. 15 The fractured bottom joint in test SSBD 3

Fig. 16 The buckled top chord in test SSBD 3

Table 7. Span dimensions of SSBD 3 (mm)

	Theory		Test	
Span	Surface Periphery	Bottom Periphery	Surface Periphery	Bottom Periphery
Span A (B)	2609	1522	2630	1580
Span C	2310	1409	2310	1345

Note: The directions of the spans are shown in Fig. 11.

free to slide horizontally and to rotate. At the last stage, due to the large deformations, all the bottom joints were raised in space, and the edge top joints became the support points. The average of the four post-tensioning forces in a cable that closed each set of five bottom chord gaps was 22 kN, which was different from that given by the finite element analyses.

The space shape of SSBD 3 is shown in Fig. 12. At the end of the test, SSBD 3 reached its maximum elastic deformation. As in SSBD 2, two continuous upper top chords yielded at four joints. Also, one bottom joint fractured due to the large shear force and a material imperfection of the connecting bolt. The fractured bottom joint also caused the buckling of a top chord. The positions of the four fractured top joints and one fractured bottom joint, as well as the failed top chord are shown in Fig. 13. The details of a fractured top and the bottom joint are shown in Figs. 14 and 15. The failed top chord is shown in Fig. 16.

The theoretical and experimental surface shapes and positions of SSBD 3 are shown in Fig. 17 (the curvature along the direction B in Fig. 11 was the same as that along direction A). The principal dimensions of SSBD 3 are listed in Table 7. It can be seen that the curvatures along the two directions A and B in Fig. 11 were the same in both the test and analyses, but different from that along direction C (with such a planar layout, uniform gaps cannot result in a part-spherical surface). From Fig. 17 it can be seen that the experimental shape of SSBD 3

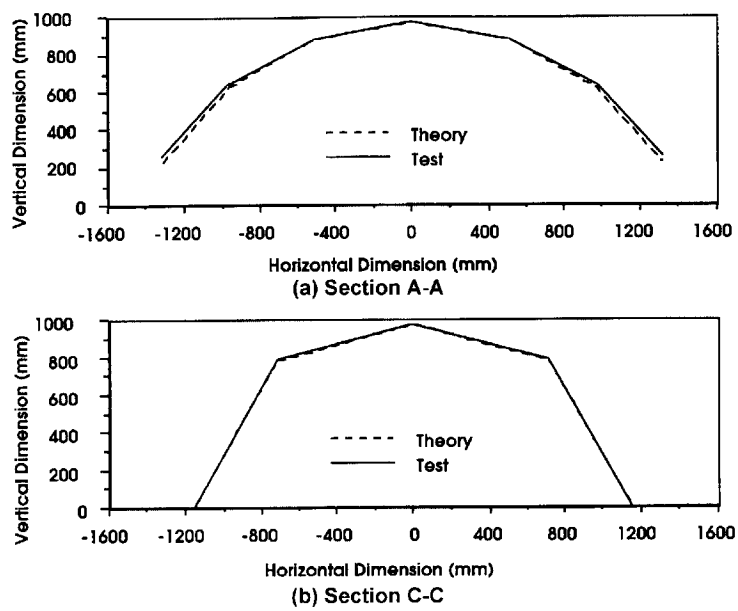

Fig. 17 Surface shapes and positions of SSBD 3 along different directions (Section A-A, B-B and C-C are defined in Fig. 11)

agrees well with the theoretical predictions. In terms of overall height, the difference between theory and test is less than 1% (the experimental overall height was 970 mm, and the theoretical overall height was 972 mm).

6. Discussion

The test results show that the post-tensioning method used in SSBD 3 can control all the exiting mechanisms. The experimental shape of SSBD 3 agrees well with the theoretical predictions (in terms of overall height, the difference between theory and test is less than 1%). This indicates that when the movements of the existing mechanisms are efficiently controlled during the post-tensioning operation, a planar layout can be deformed to a surface predicted by theoretical analysis, even if the joint stiffness is low as that in SSBD 3. Furthermore, it confirms the conclusion obtained from the test results of SSBD 2, i.e., a necessary condition to form a desired space shape from a planar layout with low joint stiffness is that the movements of all the existing mechanisms must be effectively controlled.

It was found that the fracturing of joints and the buckling of the top chord only had small effect on the space shape of SSBD 3. Except for the buckled top chord, the test dome had a smooth surface. The curvatures along the two directions A and B in Fig. 11 were almost the same (the difference was less than 5 mm). This demonstrated that such a post-tensioned and shaped dome is not sensitive to geometrical imperfections during the shape formation process. This can be attributed to the large difference between the member sizes and the overall dimensions of the dome. Due to such a large difference, the relatively small geometrical imperfections in member sizes have a neglectable effect on the space shape. Such an insensitivity to geometrical imperfections can provide economical advantages in the fabrication of post-tensioned and shaped space trusses. With a lower requirement of standards in the member tolerances than is usual for such structures, the fabrication cost will be lowered.

The test SSBD 3 reached its maximum elastic deformation extent principally due to two top chords yielding and fracturing at four joints (the fracture of the bottom joint and buckling of the top chord were an accident due to material imperfections). Because the top chords were weakened by the bolt holes at the joints, they failed at joint positions. This test confirms that the maximum elastic deformation depends on the strength of the top chords and their joints.

According to results of the finite element analyses and test, the space shape of SSBD 3 is principally determined by the post-tensioning method (i.e., positions and values of gaps). The characteristic of the top joints (e.g., pin-connected, rigid or semi-rigid) only has a very small effect on the space shape, but it affects the flexural stresses and the post-tensioning force. The finite element analysis using beam top chord elements overestimates the flexural stresses, and the analysis using rod top chord elements underestimates them. Because the maximum elastic deformation of such post-tensioned and shaped dome finally depends on the strength of the top chords, a finite element model that considers the semi-rigid characteristic of the top joints is desirable in the shape formation analysis of post-tensioned and shaped steel structures.

7. Conclusions

Based on the results of the above analyses and tests, the following conclusions can be drawn. The first two test domes, however, did not achieve the part-spherical shape as predicted by

the finite element analyses, due to the lack of control of some mechanisms. This demonstrates that when the top joints are not stiff enough, the behaviour of the truss is closer to that of a pin-connected structure. Therefore, a necessary condition to form a desired space shape from a planar layout with low joint stiffness is that the movements of all the existing mechanisms must be effectively controlled.

According to results of the finite element analyses and tests, the space shape of a post-tensioned and shaped steel dome is principally determined by the post-tensioning method (i.e., positions and values of the gaps). The stiffness characteristic of top joints (e.g., pin-connected, rigid or semi-rigid) only has a very small effect on the space shape; it only affects the flexural stresses and post-tensioning force.

The maximum elastic deformation extent of a post-tensioned and shaped steel structure is determined by the strength of the top chords and their joints. However, none of the finite element analyses using beam top chord elements or using rod top chord elements can give a close prediction for the maximum elastic deformation extent of the post-tensioned and shaped steel dome because the practical joints are semi-rigid in the test domes. While finite element analysis using beam top chord elements overestimates the flexural stresses, finite element analysis using rod top chord elements underestimates them. Therefore, a finite element program that considers the semi-rigid characteristic of the joints is desirable in the shape formation analysis of post-tensioned and shaped steel structures.

When the movements of all the existing mechanisms in the planar layout are effectively controlled, a post-tensioned and shaped dome is not sensitive to the geometrical imperfections during the shape formation process. The relatively small geometrical imperfections in member sizes have a neglectable effect on the space shape. This insensitivity to geometrical imperfections can provide an economical advantage in the fabrication of post-tensioned and shaped space trusses, due to the lower requirement of standards required for member tolerances than would be usual in space truss construction.

Acknowledgements

The research reported herein was supported by the Australian Research Council. H. Li was supported by a University of Wollongong scholarship. S. Selby fabricated the test models.

References

Calladine, C.R. (1978), "Buckminster Fuller's tensegrity structures and Clerk Maxwell's rule for the construction of stiff frames", *Int. J. of Solids Structures*, **14**(3), 161-172.

Li, H. and Schmidt, L.C. (1997), "Post-tensioned and shaped hypar trusses", *J. of Structural Engineering, ASCE*, **123**(2), 130-137.

MSC/NASTRAN User's Manual; Version 68. (1995). The MacNeal-Schwendler Corporation, Los Angeles, California, USA.

Schmidt, L.C. (1989). "Erection of space trusses of different forms by tensioning of near mechanisms", *Proc. of IASS Congress*, **4**, Madrid, Spain.

Schmidt, L.C. and Li, H. (1995a). "Geometric models of deployable metal domes", *J. of Architectural Engineering, ASCE*, **1**(3), 115-120.

Schmidt, L.C. and Li, H. (1995b). "Shape formation of deployable metal domes", *Int. J. of Space Structures*, **10**(4), 189-194.